frontiers
in Environmental Science

TYPE Original Research
PUBLISHED 27 March 2026
DOI 10.3389/fenvs.2026.1764762

# Spatiotemporal drivers of carbon footprint pressure in China's Yangtze River Economic Belt: a GTWR approach

Xin Feng[1], Ke Li[2], Liming Yang[2], Tianhao Song[3] and Tianning Wang[2]*

[1]School of Economics and Finance, Changzhou Institute of Technology, Changzhou, China, [2]School of Economics and Finance, Hohai University, Nanjing, China, [3]Business School, Hohai University, Nanjing, China

Check for updates

OPEN ACCESS

EDITED BY
Cheng Hu,
Nanjing Forestry University, China

REVIEWED BY
Dewen Liu,
Nanjing University of Posts and Telecommunications, China
Chuanhui Wang,
Qufu Normal University, China

*CORRESPONDENCE
Tianning Wang,
2263510323@hhu.edu.cn

RECEIVED 10 December 2025
REVISED 05 March 2026
ACCEPTED 10 March 2026
PUBLISHED 27 March 2026

CITATION
Feng X, Li K, Yang L, Song T and Wang T (2026) Spatiotemporal drivers of carbon footprint pressure in China's Yangtze River Economic Belt: a GTWR approach. *Front. Environ. Sci.* 14:1764762. doi: 10.3389/fenvs.2026.1764762

As a critical engine of China's economic growth and ecological security, the Yangtze River Economic Belt (YREB) faces the dual challenge of sustaining development while mitigating carbon footprint pressure (CFP). This study examines the driving forces and spatiotemporal heterogeneity of CFP in the YREB from 2000 to 2021, aiming to support the region's contribution to the United Nations Sustainable Development Goals. By integrating an extended STIRPAT model with Geographically and Temporally Weighted Regression (GTWR) and General Dominance Analysis (GDA), we isolate the specific contributions of population, affluence, and technology. The results indicate that: (1) economic inertia remains the dominant stressor, with population growth and economic expansion significantly increasing CFP, outweighing the mitigation effects of energy efficiency improvements; (2) the industrial structure has shifted roles, transitioning from a primary driver of carbon pressure to an inhibitor in later years, reflecting effective policy interventions in the tertiary sector; and (3) spatial heterogeneity is pronounced, with the midstream region identified as the critical "governance bottleneck" due to high industrial intensity, whereas the downstream region exhibits advanced decoupling trends. These findings suggest that single-dimensional energy transitions are insufficient for the YREB; a differentiated regional strategy focusing on midstream industrial upgrading is essential for achieving carbon neutrality.

KEYWORDS
**carbon footprint pressure, GTWR model, SDG7, STIRPAT model, Yangtze River Economic Belt**

## 1 Introduction

The global imbalance between carbon emissions and natural sinks has become one of the defining challenges of the 21st century. For rapidly industrializing economies, the tension between sustaining economic growth and respecting planetary boundaries is particularly acute. The United Nations Sustainable Development Goals (SDGs), specifically SDG7 (Affordable and Clean Energy) and SDG13 (Climate Action), provide a framework for navigating this trade-off (Charles and Emrouznejad, 2024). While SDG7 encompasses energy affordability, accessibility, and cleanliness, this study primarily focuses on the renewable energy transition dimension due to its direct impact on carbon mitigation.

China, as a key participant in global climate governance, has committed to ambitious "dual carbon" goals. Central to this strategy is the Yangtze River Economic Belt (YREB), a region that serves as China's "dual engine" for both economic output and ecological conservation. Although the YREB covers only 21% of China's land area and has a forest coverage rate of 41.3%, it generates over 40% of the national GDP and accounts for approximately 30% of total $CO_2$ emissions (Wu et al., 2023). This disparity highlights a critical spatial mismatch: carbon sinks are concentrated in the less developed western and southern regions, while emissions are clustered in the industrialized eastern and northern areas (Huang et al., 2023).

To scientifically assess this imbalance, Carbon Footprint Pressure (CFP) has emerged as a superior metric compared to simple carbon emissions, as it integrates both the generation of carbon (sources) and the ecosystem's capacity to absorb it (sinks) (Chen et al., 2020). Unlike indicators that merely reflect the scale of emissions, CFP characterizes the relative extent to which emissions occupy ecological absorption capacity. Its variation depends on both emission expansion and the constraints imposed by carbon sinks, thereby enabling the identification of ecological deficits within regions. While previous studies have extensively utilized frameworks such as the Environmental Kuznets Curve (EKC) (Grossman and Krueger, 1995) and the STIRPAT model (York et al., 2002) to identify drivers of emissions, few have applied these rigorous tools to the ratio of emissions to sink capacity (CFP) in a spatially explicit manner.

Existing literature on the YREB has largely established that economic scale is the primary driver of emission growth (Ma et al., 2019; Wang Z. et al., 2021), while technological progress serves as a moderating factor (Chen et al., 2023). However, three critical gaps remain. First, most studies treat the YREB as a homogeneous unit or focus on static "average" drivers, overlooking the dynamic spatiotemporal heterogeneity among the upstream, midstream, and downstream regions (Zhang and Lei, 2023). Second, the interaction between energy transition (SDG7) and ecological carrying capacity is rarely quantified within a unified model. Third, research methodologies often lack sufficient precision to identify non-stationary variations of different drivers across temporal and spatial dimensions. Existing spatial econometric studies predominantly employ Spatial Durbin Models (SDM) or Spatial Error Models (SEM) to characterize spatial dependency structures. These models identify spatial spillover effects by incorporating spatial lag terms but typically assume global spatial stability of regression parameters (Yang et al., 2021). In contrast, Geographically Weighted Regression (GWR) and its extension, Geographically and Temporally Weighted Regression (GTWR), introduce a kernel weighting mechanism that allows regression coefficients to vary continuously across spatial and temporal dimensions (Huang et al., 2010). Their estimation outcomes depend on the form of the weighting kernel and the bandwidth selection strategy, with bandwidth settings directly impacting the model's parameter identifiability and estimation stability (Guo et al., 2008). Therefore, given the distinct regional development stages and potential non-stationarity in driving mechanisms, it is necessary to introduce analytical frameworks capable of capturing local parameter dynamics. This should be done after discerning the theoretical differences among various spatial econometric models.

This study addresses existing gaps by examining the drivers of CFP in the YREB from 2000 to 2021. We develop an integrated "STIRPAT-GDA-GTWR" framework to achieve three objectives: (1) quantify the contributions of population, affluence, and technology to CFP using General Dominance Analysis (GDA); (2) identify the spatiotemporal heterogeneity of these drivers through Geographically and Temporally Weighted Regression (GTWR); and (3) assess the region's decoupling potential under the constraints of SDG7. By moving beyond regional-level averages to provincial-level dynamics, this research provides granular evidence base essential for differentiated regional policymaking aimed at achieving China's carbon neutrality targets.

## 2 Materials and methods

### 2.1 Calculation of carbon footprint pressure (CFP)

To assess the environmental stress caused by economic activities in a region, we use the Carbon Footprint Pressure (CFP) index. The CFP is defined as the ratio of regional carbon emissions ($C$) to the region's carbon absorption capacity ($CA$).

$$CFP = C/CA$$

where $C$ represents the apparent carbon emissions derived from energy consumption and industrial processes. The carbon absorption capacity ($CA$) focuses on terrestrial ecosystems. Since forestland accounts for over 96% of the total carbon sink in the YREB, we adopt a conservative estimation approach by using forest carbon sequestration as a proxy for the total regional sink capacity. While this proxy captures the vast majority of the region's sink capacity, it inevitably excludes contributions from soil, wetlands, and croplands. This conservative approach may result in certain measurement discrepancies in highly diverse ecological areas, a limitation that is further discussed in the Limitations and Future Prospects section. The calculation is based on the methodology of Song et al. (2021):

$$CA = a \times S/0.96$$

where $S$ denotes the forest area ($hm^2$), and $a$ is the average carbon absorption coefficient, set at 3.8096 t/($hm^2$·a).

### 2.2 The STIRPAT-GDA-GTWR framework

To identify the drivers of CFP, we extend the stochastic STIRPAT model. We decompose the environmental impact ($I$) into Population ($P$), Affluence ($A$), and Technology ($T$), further expanding the Technology component to capture the specific industrial and energy characteristics of the YREB. The extended model is expressed as follows:

$$\ln CFP = a + b \ln PS + c \ln GP + d_1 \ln SR + d_2 \ln TR + e_1 \ln EI + e_2 \ln ES + e$$

where $PS$ is the population size; $GP$ is *per capita* GDP; $SR$ and $TR$ represent the shares of secondary and tertiary industries, respectively; $EI$ is energy intensity (energy/GDP); and $ES$ is the renewable energy structure.

To ensure robustness and effectively capture spatial dynamics, we employ a two-step analytical process.

TABLE 1 **Variable overview.**

| Variable | Meaning | Measurement | Data source |
|---|---|---|---|
| CFP | Carbon footprint pressure | Ratio of regional carbon emissions to regional carbon sinks | CEADs database |
| PS | Population size | Year-end population statistics | CSMAR database |
| GP | Gross product per capita | Total GDP/Population size | CSMAR database |
| SR | Secondary industry ratio | Secondary industry GDP/Total GDP | CSMAR database |
| TR | Tertiary industry ratio | Tertiary industry GDP/Total GDP | CSMAR database |
| EI | Energy intensity | Energy consumption/Total GDP | China energy statistical yearbook and the statistical yearbooks of each province |
| ES | Energy structure | The proportion of total electricity generation from renewable energy sources | China electric power statistical yearbook |

The original values of SR, and TR, have been converted to integer percentages (e.g., 30 represents 30%) before taking the logarithm.

1. General Dominance Analysis (GDA): We first employ GDA to address multicollinearity and rank the relative importance of each variable based on its contribution to the model's $R^2$ (Luchman, 2021).
2. Geographically and Temporally Weighted Regression (GTWR): To address the spatial non-stationarity inherent in the YREB, we extend the traditional GWR model by incorporating a temporal dimension. The GTWR model enables regression coefficients to vary across both space and time:

$$ln(CFP_{it}) = \beta_0(u_i, v_i, t_i) + \sum_{k=1}^{p} \beta_k(u_i, v_i, t_i) X_{k,it} + e_{it}$$

where $(u_i, v_i, t_i)$ denotes the spatiotemporal coordinates of province $i$ at year $t$.

# 3 Data

This study utilizes a panel dataset encompassing the 11 provinces of the Yangtze River Economic Belt (YREB) from 2000 to 2021. Socioeconomic indicators—including population size (PS), GDP (GP), and industrial structure (SR, TR)—were obtained from the CSMAR database and the National Bureau of Statistics, with GDP figures adjusted to constant prices to account for inflation. Data on apparent carbon emissions were sourced from the Carbon Emission Accounts and Datasets (CEADs), while forest area data were retrieved from the China Forestry Information Network. Energy intensity (EI) was calculated using data from the China Energy Statistical Yearbook. Due to the lack of provincial-level renewable energy consumption data, the energy structure (ES) was approximated by the ratio of renewable electricity generation (hydro, wind, and solar) to total electricity generation, following the methodology of Wang J. et al. (2021) and Bao and Xu (2019). Although this proxy effectively captures the clean energy transition within the power sector, we acknowledge that it does not fully represent non-electric energy consumption, such as industrial fuels and heating; the implications of this limitation are discussed in the study. Finally, latitude and longitude coordinates for administrative centers were obtained from GeoJSON (https://geojson.cn/) to support spatial analysis. Table 1 provides an overview of each variable.

Table 2 summarizes the basic characteristics of the data. Among all the data series, lnGP has the highest mean, while lnEI has the lowest mean value. lnES exhibits the highest standard deviation, indicating that the energy structure (i.e., the proportion of renewable energy generation in total power generation) is the most variable. In contrast, lnSR has the lowest standard deviation, suggesting it is the most stable variable among all the data series. The Jarque–Bera (J-B) normality test reveals that, except for lnEI, the data for all other variables deviate significantly from a normal distribution, as indicated by the highly significant test statistics.

Table 3 presents the correlation matrix for the panel variables. The statistics indicate that the correlations between lnCFP and the other variables, except for lnSR, are highly significant and exhibit relatively strong correlation coefficients.

# 4 Results and discussion

## 4.1 Temporal evolution of carbon footprint pressure (CFP)

To evaluate the environmental stress caused by regional economic activities, this study calculated the Carbon Footprint Pressure (CFP) index, defined as the ratio of carbon emissions to carbon sinks, using the forest sink proxy method established in previous research. Figure 1 depicts the temporal evolution of CFP across the Yangtze River Economic Belt (YREB) and its three major sub-regions from 2000 to 2021. The results reveal a persistent "ecological deficit," with CFP values consistently exceeding 1, indicating that carbon emissions in the region significantly surpass its carbon absorption capacity. This trend corroborates the findings of Huang et al. and others (Huang et al., 2021; Tian et al., 2024; Fan et al., 2022; Liang et al., 2022), confirming that rapid

TABLE 2 Summary statistics.

| Variable | Mean | SD | Min | Max | Jarque-Bera test |
|---|---|---|---|---|---|
| lnCFP | 2.484 | 1.645 | −0.190 | 7.410 | 67*** |
| lnPS | 8.497 | 0.403 | 7.386 | 9.074 | 21.58*** |
| lnGP | 10.07 | 0.975 | 7.798 | 11.99 | 11.06*** |
| lnSR | 3.773 | 0.137 | 3.265 | 4.076 | 12.93*** |
| lnTR | 3.754 | 0.172 | 3.387 | 4.299 | 19.07*** |
| lnEI | −0.129 | 0.584 | −1.232 | 1.543 | 4.187 |
| lnES | 2.436 | 2.484 | −11.51 | 4.521 | 2,570*** |

$^{***}p < 0.01$, $^{**}p < 0.05$, $^{*}p < 0.1$. To avoid undefined mathematical operations (ln 0) during the logarithmic transformation, a small constant ($10^{-5}$) was added uniformly to all raw observations of the energy structure (ES) variable. This standard econometric adjustment addresses the negative minimum value of lnES, observed in the dataset.

TABLE 3 Correlation matrix.

| Variables | lnCFP | lnPS | lnGP | lnSR | lnTR | lnEI | lnES |
|---|---|---|---|---|---|---|---|
| lnCFP | 1 | | | | | | |
| lnPS | −0.39*** | 1 | | | | | |
| lnGP | 0.54*** | −0.09 | 1 | | | | |
| lnSR | 0.05 | 0.28*** | −0.04 | 1 | | | |
| lnTR | 0.51*** | −0.33*** | 0.74*** | −0.54*** | 1 | | |
| lnEI | −0.34*** | −0.09 | −0.92*** | 0.05 | −0.66*** | 1 | |
| lnES | −0.78*** | 0.38*** | −0.18*** | −0.20*** | −0.15** | 0.05 | 1 |

$^{***}p < 0.01$, $^{**}p < 0.05$, $^{*}p < 0.1$.

industrialization has increasingly strained the ecological environment.

When evaluated regionally, the data reveal a clear spatial gradient in which CFP progressively increases from the upstream to the downstream regions. Despite its advanced economic status, the downstream region experiences the highest environmental pressure, followed by the midstream region. Specifically, Shanghai has seen a decline in CFP since approximately 2003; however, its absolute value remains high due to population density and limited vegetation coverage. In contrast, the upstream region functions as an ecological barrier, although internal disparities are emerging. While Yunnan maintains a relatively low CFP owing to its extensive forest resources, Guizhou exhibits a sustained increase, and Chongqing shows significant fluctuations. These disparities highlight the complex challenges of achieving balanced development, as varying economic models and ecological carrying capacities create distinct pressure points across the basin.

## 4.2 Econometric model verification

Before interpreting the driver analysis, it is essential to verify the statistical robustness of the panel data. We conducted a comprehensive series of diagnostic tests, including multicollinearity (VIF), unit root (CIPS), cointegration (Kao and Pedroni), and cross-sectional dependence (CD) tests. The detailed results of these diagnostics are presented in Supplementary Tables S1–S5. The tests confirmed that the data series are stationary at the first difference and exhibit a long-term cointegration relationship. Furthermore, due to the detection of significant heteroscedasticity and serial autocorrelation, the Panel-Corrected Standard Error (PCSE) estimation method was chosen over standard OLS to ensure the validity and reliability of the regression analysis.

## 4.3 Global drivers and contribution analysis

To quantify the specific contributions of socioeconomic factors to CFP, we employed the extended STIRPAT model using PCSE estimation and General Dominance Analysis (GDA). Table 4 presents the regression coefficients, while Table 5 ranks the variables according to their contribution to the model's goodness of fit. Consistent with the Environmental Kuznets Curve (EKC) hypothesis and national-level studies, the results indicate that economic scale and industrial structure are the primary stressors. Specifically, *per capita* GDP (GP) and the proportion of secondary industry (SR) exhibit high positive elasticities of 0.681 and 0.845, respectively ($p < 0.01$). This suggests that growth in the YREB remains heavily reliant on energy-intensive industrialization.

In terms of mitigation, the energy structure (ES) exhibits a significant inhibitory effect, with a coefficient of −0.108. This finding confirms that increasing the share of renewable energy is an effective strategy for reducing CFP, aligning with the objectives of SDG7. However, the GDA results reveal a critical hierarchy in driver dominance: economic development (GP) is the most influential variable, contributing approximately 40% to the model's explanatory power (Rank 1), whereas population size (PS) contributes minimally (Rank 6). This low contribution of population contrasts with early development stages but aligns with observations in highly urbanized regions, where infrastructure and land-use policies have stabilized demographic impacts. Consequently, the "scale effect" of the economy currently outweighs the "technological effect" of the energy transition, underscoring the need for more aggressive structural adjustments.

## 4.4 Temporal heterogeneity of influencing factors

Moving beyond global averages, the Geographically and Temporally Weighted Regression (GTWR) model captures the

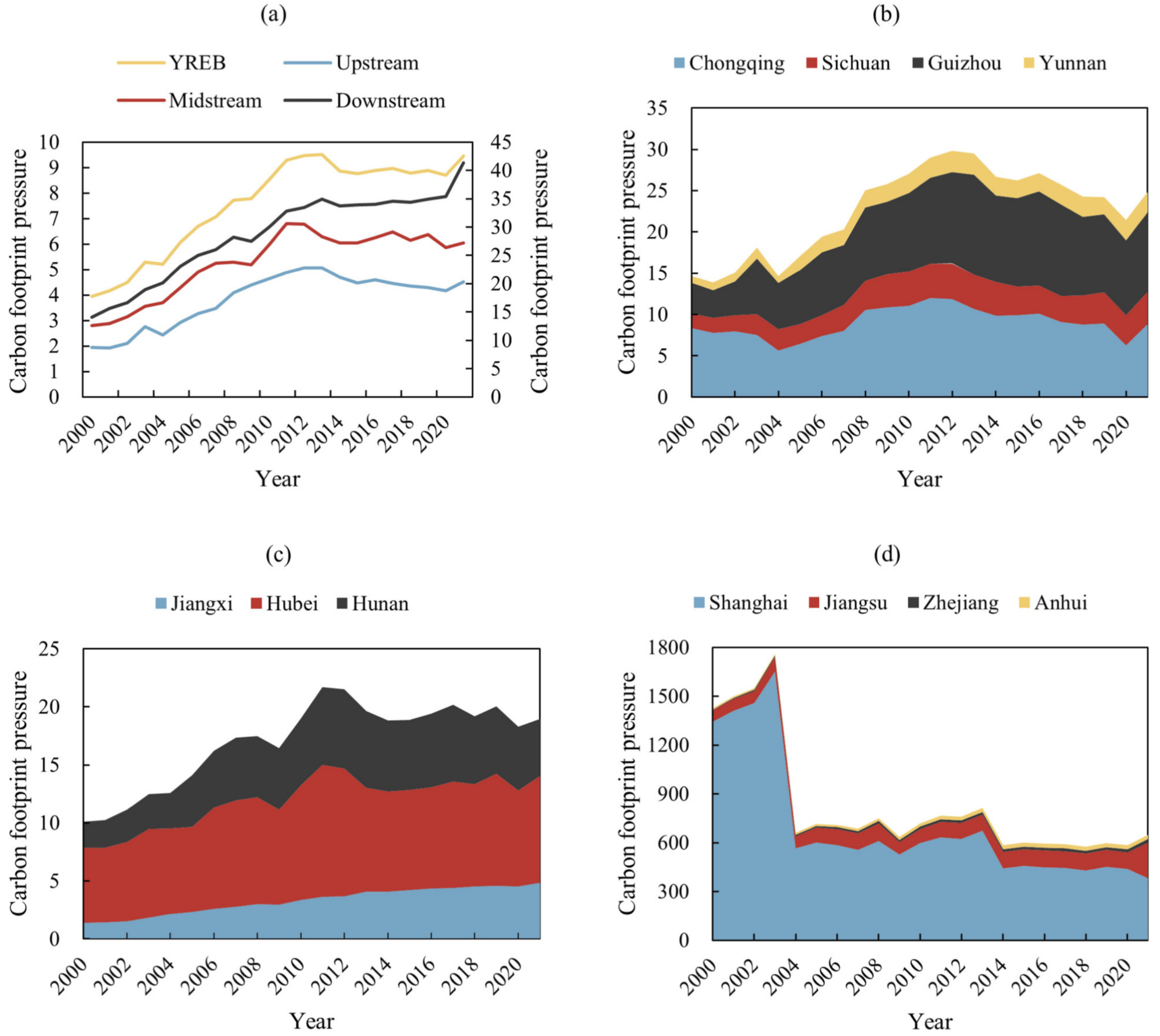

FIGURE 1
CFP trends in the YREB from 2000 to 2021. Figure 1a shows the changing trends of the CFP for the entire YREB and its upper, middle, and lower reaches, with the curve for the lower reaches specifically plotted against the right axis. Figures 1b–d displays the changing trends of the CFP in the provinces of the upper, middle, and lower reaches, respectively.

dynamic evolution of these drivers over time. The model parameters are presented in Table 6, where both $R^2$ and adjusted $R^2$ exceed 0.95. This indicates a high level of model fit, demonstrating strong explanatory power. Consequently, the model results effectively elucidate the spatiotemporal heterogeneity of the impacts of various factors.

Figure 2 illustrates the time-series variation of the average regression coefficients from 2000 to 2021. These trends exhibit significant temporal heterogeneity, reflecting the influence of evolving policy landscapes. Most notably, the "M-shaped" fluctuation observed in the SR coefficient, particularly the inflection points around 2008 and 2014, closely corresponds to the implementation periods of China's 11th Five-Year Plan (2006–2010) and 12th Five-Year Plan (2011–2015). The 11th Five-Year Plan introduced, for the first time, binding environmental targets linked to local officials' performance assessments (Wang and Xu, 2022), including a 20% reduction in energy intensity per unit of GDP and a 10% reduction in major pollutant emissions. These mandatory targets transformed environmental regulation from a "soft constraint" into a "hard constraint." During the 12th Five-Year Plan period, the policy focus shifted toward promoting green transformation, with explicit requirements to phase out backward production capacity in 13 high-energy-consuming industries—including coal, power, and steel—and to implement differentiated electricity pricing policies. This temporal alignment suggests that macroeconomic policy interventions likely influenced this trend. Han et al. (2017) demonstrated that the binding pollution control targets introduced during the 11th Five-Year Plan had significant regulatory addition, pollution reduction, and resource misallocation correction effects,

TABLE 4 **Panel-corrected standard error (PCSE) findings.**

| Variable | lnCFP |
|---|---|
| lnPS | 0.683*** |
|  | (4.02) |
| lnGP | 0.681*** |
|  | (13.31) |
| lnSR | 0.845*** |
|  | (5.40) |
| lnTR | 0.696*** |
|  | (4.53) |
| lnEI | 0.760*** |
|  | (9.27) |
| lnES | −0.108*** |
|  | (-13.53) |
| Constant | −15.259*** |
|  | (-7.91) |
| Observations | 242 |
| Number of provinces | 11 |
| R-squared | 0.992 |
| Province fixed effects | Yes |
| Mean VIF | 5.09 |
| Wald $\chi^2$ | 106,827.87*** |

***$p < 0.01$, **$p < 0.05$, *$p < 0.1$.

substantially improving productivity in regulated industries. Wu and Deng (2018) found that environmental regulation exerted a significant negative inhibitory effect on the agglomeration of high-energy-consuming industries in the Yangtze River Economic Belt, with the share of such industries' output value declining during the 12th Five-Year Plan period. Furthermore, Luo and Qi (2021), using the water pollution control policy in the 11th Five-Year Plan as an exogenous shock, provided robust evidence that stringent environmental regulation in the Yangtze River Basin significantly drove industrial transfer and upgrading. These findings corroborate our observation that the inflection points in the SR coefficient are likely linked to the stringent environmental targets enforced during these plans.

Similarly, the influence of energy intensity (EI) follows a "rise-then-fall" trajectory, peaking in 2011 before declining into negative values by 2017. This pattern reflects the characteristics of the EKC, suggesting that improvements in energy efficiency have begun to suppress CFP after surpassing a certain development threshold. In contrast, the coefficient for the tertiary industry (TR) exhibits a consistent downward trend, eventually becoming negative. This indicates successful structural optimization, with the service sector gradually transitioning toward low-carbon models. However, the energy structure (ES) coefficient, while consistently negative, remains relatively stable. This suggests that although renewable energy adoption is beneficial, its current linear growth rate is insufficient to disrupt the dominant carbon-intensive dependencies; an exponential acceleration is necessary to enhance its mitigating impact.

## 4.5 Spatial heterogeneity of influencing factors

To address the spatial non-stationarity inherent in the YREB, the GTWR model further decomposes the drivers by region. Figure 3 illustrates the spatial distribution of the regression coefficients, revealing a "center-periphery" divergence in driver sensitivity.

To robustly quantify this spatial heterogeneity and address potential localized sample fluctuations, independent t-tests were conducted on the regional average coefficients (Table 7). The statistical results provide strong quantitative support for the "Midstream Trap" hypothesis. The data reveal that the midstream provinces (Hubei, Jiangxi, and Hunan) are trapped in a highly resource-dependent development phase, exhibiting significantly greater sensitivities to key emission stressors than the rest of the basin. Specifically, the midstream's sensitivity to energy intensity (lnEI mean = 2.200) is more than three times higher than both the downstream (0.642) and upstream (0.649) averages, with differences statistically significant at the 1% level ($p < 0.001$). Furthermore, its vulnerability to population expansion (lnPS mean = 0.783) and economic scale (lnGP mean = 1.905) significantly exceeds that of both the upstream ($p < 0.001$) and downstream ($p < 0.05$) regions. For instance, Hubei Province exhibits extreme local stress, with an energy intensity coefficient peaking at 2.279 and a population size coefficient of 0.850. Although

TABLE 5 **General dominance statistics.**

| lnCFP | Dominance stat. | Standardized domin. stat. | Ranking |
|---|---|---|---|
| lnGP | 0.0129 | 0.3969 | 1 |
| lnEI | 0.0068 | 0.2084 | 2 |
| lnES | 0.0053 | 0.1616 | 3 |
| lnSR | 0.0039 | 0.1195 | 4 |
| lnTR | 0.003 | 0.0918 | 5 |
| lnPS | 0.0007 | 0.0218 | 6 |

TABLE 6 Parameters of the GTWR model.

| Indicator | Parameter | Indicator | Parameter |
|---|---|---|---|
| Bandwidth | 0.115 | $R^2$ | 0.9788 |
| Residual squares | 13.874 | Adjusted $R^2$ | 0.9783 |
| Sigma | 0.2394 | Spatiotemporal distance ratio | 0.6461 |
| AICc | 148.91 | Trace of spatial matrix | 56.8857 |

population size has the lowest global contribution in the GDA ranking, its pronounced impact in Hubei reveals a unique regional urbanization mechanism. Unlike the downstream regions, where population agglomeration is absorbed by low-carbon service sectors and mature infrastructure, Hubei—centered around the rapid expansion of the Wuhan Metropolitan Area—has experienced massive demographic inflows that trigger large-scale, carbon-intensive urban construction (e.g., housing, subways, and bridges). Furthermore, because Hubei serves as a traditional heavy industry base dominated by automotive manufacturing, metallurgy, and building materials (Zhang and Lei, 2023), population growth directly translates into rigid demands for high-carbon products and residential energy. This overlapping effect of a heavy-industrial structure and rapid urbanization locks the midstream region into a resource-dependent development phase, lacking the advanced efficiency of the downstream or the ecological buffer of the upstream.

Conversely, the downstream region, led by Shanghai, exhibits the lowest sensitivity to these scale factors (Shanghai population coefficient: 0.156; energy intensity coefficient: 0.115). This observation aligns with the characteristics of a post-industrial economy, where infrastructure is mature and growth is decoupled from physical resource consumption. An intriguing anomaly is observed in the upstream province of Yunnan, which displays the highest positive coefficient for the tertiary industry (1.080). This finding strongly challenges the conventional view that “services are inherently green.” A closer examination of Yunnan’s economic structure reveals two specific sub-sectoral drivers responsible for this anomaly. First, Yunnan relies heavily on tourism as its pillar industry. Due to its rugged mountainous terrain, the province’s tourism sector depends significantly on carbon-intensive aviation and highway passenger transport, which substantially increases the region’s carbon footprint (Gössling and Peeters, 2015). Second, under China’s “East Data, West Computing” initiative, Yunnan has aggressively expanded its digital economy by hosting numerous large-scale data centers (Xie et al., 2024). Although these facilities belong to the tertiary sector, they function as “smokeless steel mills,” requiring massive and continuous electricity consumption for server operation and cooling. During dry seasons, when local hydropower is insufficient, this structural shift necessitates reliance on fossil-fuel backup power. This situation underscores the urgent need for sub-sector-specific decarbonization strategies in upstream regions.

To rigorously assess the statistical reliability of the spatially varying coefficients and to address potential local sample

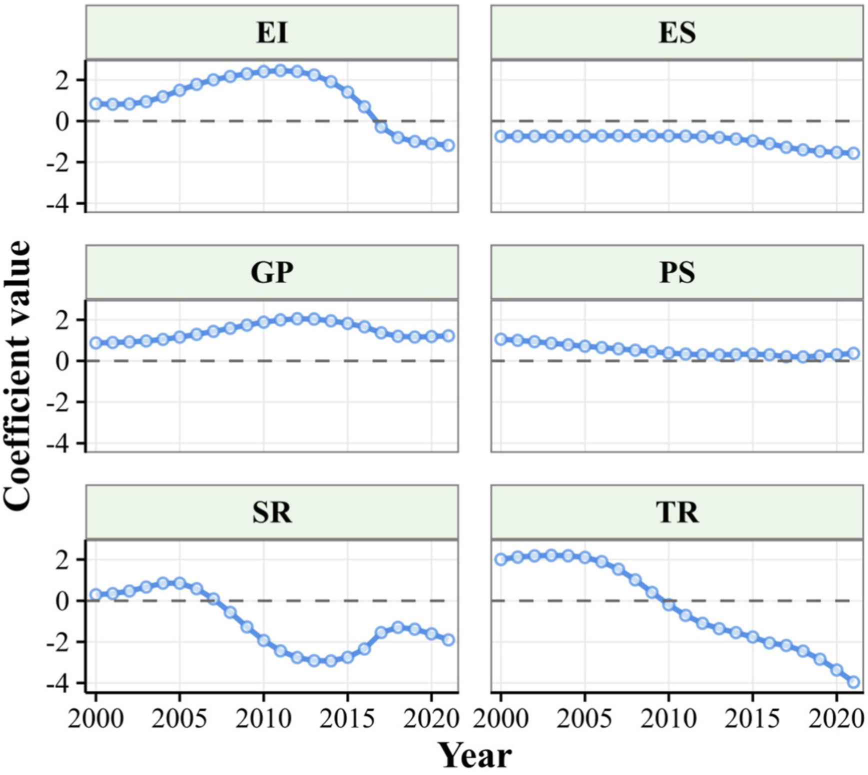

FIGURE 2
Time series variation in average regression coefficients for influencing factors of CFP in the YREB from 2000 to 2021.

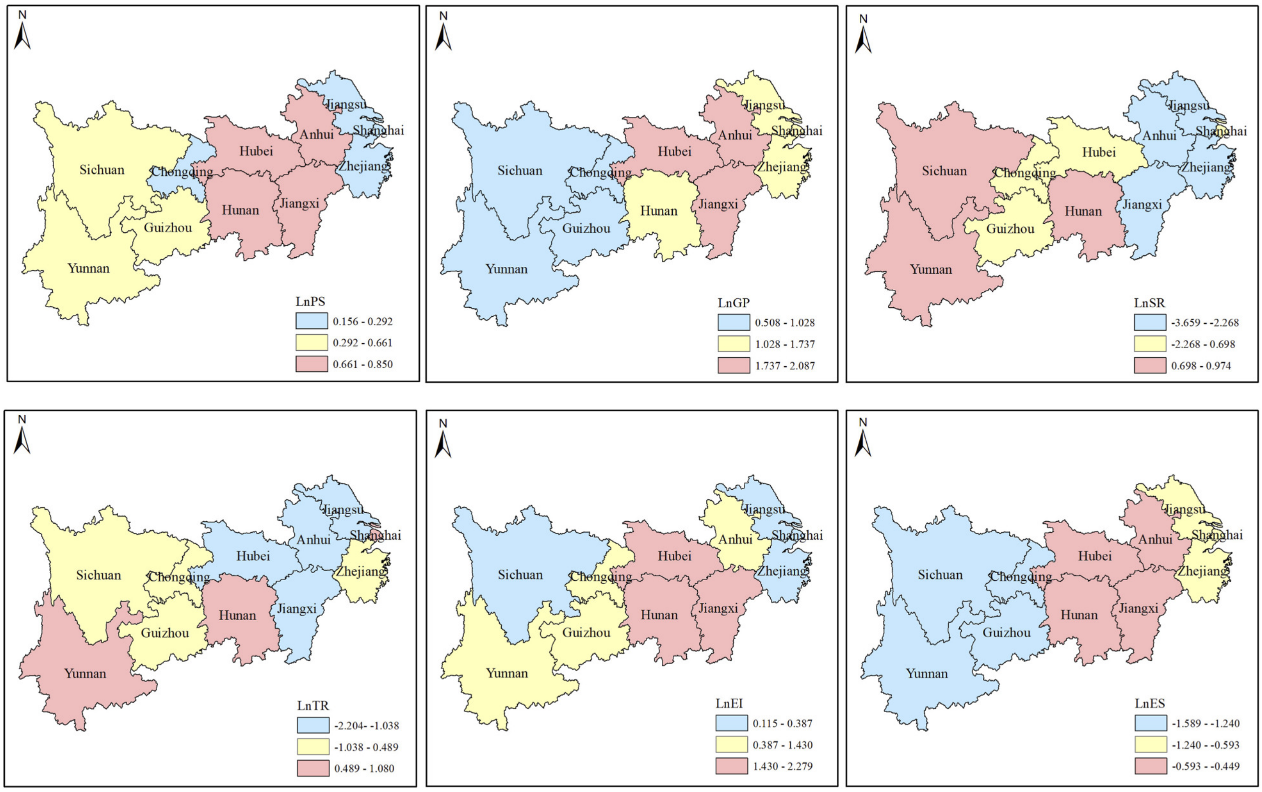

FIGURE 3
Spatial distribution of average regression coefficients for influencing factors of CFP in the YREB.

TABLE 7 **Regional comparison of GTWR average coefficients and significance of differences.**

| Variables | Upstream (mean ± SD) | Midstream (mean ± SD) | Downstream (mean ± SD) | Mid vs. Down (*p* -value) | Mid vs. Up (*p* -value) |
|---|---|---|---|---|---|
| lnPS | 0.497 ± 0.261 | 0.783 ± 0.326 | 0.344 ± 0.756 | 0.000*** | 0.000*** |
| lnGP | 0.643 ± 0.499 | 1.905 ± 0.816 | 1.616 ± 1.018 | 0.040 | 0.000*** |
| lnSR | 0.842 ± 0.916 | −1.481 ± 3.915 | −1.963 ± 4.098 | 0.438 | 0.000*** |
| lnTR | 0.674 ± 1.138 | −0.826 ± 3.806 | −0.494 ± 3.239 | 0.555 | 0.003*** |
| lnEI | 0.649 ± 0.427 | 2.200 ± 0.620 | 0.642 ± 3.372 | 0.000*** | 0.000*** |
| lnES | −1.464 ± 0.275 | −0.534 ± 0.181 | −0.854 ± 0.598 | 0.000*** | 0.000*** |

***$p < 0.01$, **$p < 0.05$, *$p < 0.1$. P-values are derived from two-tailed independent T-tests. The midstream region includes Hubei, Hunan, and Jiangxi. the coefficients represent the spatiotemporal sensitivity of carbon footprint pressure to each driving factor.

fluctuations, a Time-Significance Coverage Heatmap was constructed (Figure 4). This heatmap displays the proportion of years (2000–2021) during which each local GTWR coefficient was statistically significant at the 10% level.

The results strongly validate our core spatial findings. Most notably, the variables defining the "Midstream Trap"—economic scale (lnGP), energy intensity (lnEI), and population size (lnPS) in Hubei, Hunan, and Jiangxi—exhibit exceptionally high temporal robustness, with coverage predominantly ranging from 95% to 100%. This confirms that the severe resource dependence and carbon footprint pressures in the midstream region have been persistent structural realities over the past 2 decades, rather than temporary artifacts of bandwidth smoothing. Furthermore, energy structure (lnES) consistently demonstrates 100% significance coverage across all provinces, underscoring the universal and enduring importance of renewable energy transitions throughout the study period.

Interestingly, the heatmap also reveals nuanced regional development phases through variations in significance coverage. For example, while the secondary industry (lnSR) demonstrates highly robust impacts in the heavily industrialized midstream and downstream regions, its lower significance coverage in Yunnan

| | lnPS | lnGP | lnSR | lnTR | lnEI | lnES |
|---|---|---|---|---|---|---|
| Shanghai | 95% | 95% | 100% | 91% | 91% | 100% |
| Jiangsu | 95% | 100% | 64% | 100% | 95% | 100% |
| Zhejiang | 95% | 77% | 100% | 73% | 82% | 100% |
| Anhui | 100% | 100% | 82% | 95% | 91% | 100% |
| Jiangxi | 100% | 100% | 95% | 95% | 100% | 100% |
| Hubei | 100% | 100% | 95% | 91% | 100% | 100% |
| Hunan | 100% | 100% | 64% | 64% | 100% | 100% |
| Chongqing | 32% | 82% | 55% | 59% | 68% | 100% |
| Sichuan | 100% | 77% | 55% | 32% | 41% | 100% |
| Guizhou | 73% | 86% | 77% | 82% | 86% | 100% |
| Yunnan | 100% | 59% | 23% | 41% | 77% | 100% |

FIGURE 4
Significance coverage heatmap of local GTWR coefficients by province (2000–2021).

(23%) reflects the province’s distinct economic structure, where heavy manufacturing has historically played a smaller role in driving carbon footprint pressure. Similarly, the partial significance of the tertiary sector (lnTR) in Yunnan (41%) aligns with the fact that its carbon-intensive tertiary activities (e.g., big data centers and mass tourism) are relatively recent phenomena emerging in the latter half of the study period, characterizing them as emerging drivers rather than long-standing historical baselines. This temporal heterogeneity further underscores the necessity of differentiated, phase-specific decarbonization strategies across the YREB.

## 5 Conclusion

This study integrates an extended STIRPAT framework with General Dominance Analysis (GDA) and Geographically and Temporally Weighted Regression (GTWR) to analyze the driving mechanisms of Carbon Footprint Pressure (CFP) in the Yangtze River Economic Belt (YREB) from 2000 to 2021. The investigation produces three primary conclusions concerning the region’s progress toward the Sustainable Development Goals (SDGs).

First, the interplay between economic inertia and the energy transition reveals a “relative decoupling” rather than an absolute one. Although the expansion of renewable energy (SDG7) and improvements in energy intensity have significantly mitigated CFP, these gains are currently insufficient to offset the environmental burden caused by the scale effects of population agglomeration and economic growth. Dominance analysis confirms that economic expansion remains the primary stressor, creating a “structural carbon lock-in” where the marginal benefits of single-dimensional energy transitions diminish in the face of rapid GDP growth.

Second, the temporal evolution of these drivers exhibits distinct policy-driven heterogeneity. The influence of the secondary industry on CFP displayed a characteristic “M-shaped” volatility, while energy intensity followed a “rise-then-fall” trajectory. These inflection points coincide with the implementation of stringent environmental regulations during China’s Five-Year Plans, indicating that government intervention has been effective in enforcing threshold-based structural adjustments. However, the stability of the population and energy structure coefficients suggests that demographic factors and the fundamental energy mix possess high inertia and require long-term, consistent governance rather than short-term interventions.

Third, spatial heterogeneity analysis reveals a critical “Midstream Trap.” The driving forces behind CFP—particularly industrial structure and energy intensity—are significantly stronger in the midstream provinces (e.g., Hubei, Jiangxi) compared to the downstream or upstream regions. This suggests that the midstream region has become a “pollution haven” or a bottleneck in the basin’s green development, lacking the advanced tertiary sector decoupling seen in Shanghai while also missing the ecological buffer advantages of the western region. Furthermore, the upstream region exhibits unique anomalies; specifically, the tertiary industry in Yunnan acts as a carbon driver rather than a sink, likely due to the energy demands of the digital economy and tourism-related transport. This challenges the assumption that growth in the service sector is inherently low-carbon.

## 6 Policy recommendations

Based on the multidimensional and spatially heterogeneous drivers identified above, we propose a differentiated governance strategy to promote the synergistic development of both the economy and the environment.

Prioritize addressing the “Midstream Trap” through cross-regional collaboration and targeted retrofitting of heavy industries. Since the midstream region exhibits the highest sensitivity to carbon drivers, it should be designated as the primary focus area for CFP governance. A tailored approach is necessary, whereby downstream provinces (e.g., Shanghai, Jiangsu), which have achieved a higher level of decoupling, provide technological and financial support to the midstream region. Specifically, the establishment of a basin-wide horizontal ecological compensation mechanism is recommended. However, rather than generic industrial upgrading, these compensation funds must be allocated to specific high-energy sub-sectors. Given Hubei's extreme sensitivity to energy intensity, local governments must enforce strict capacity replacement policies and implement "Top Runner" energy efficiency benchmarks targeting its key heavy industries: steel, metallurgy, automotive manufacturing, and building materials (e.g., cement). Subsidies from downstream beneficiaries should directly finance low-carbon technology retrofits (e.g., electric arc furnaces for steelmaking) in these sectors, thereby mitigating the "pollution haven" effect and breaking the structural carbon lock-in observed in Hubei and Jiangxi.

Differentiate sectoral policies to address upstream anomalies. In the upstream regions, particularly Yunnan and Guizhou, policy focus must shift from broad industrial suppression to targeted sectoral decarbonization. Given that the tertiary industry is the primary driver of emissions in these areas, policymakers should enforce stringent green energy consumption standards for emerging digital infrastructure (e.g., data centers under the "East Data, West Computing" initiative) and promote the electrification of tourism transportation. To operationalize this, local authorities should establish a strict Power Usage Effectiveness (PUE) threshold for all newly approved data centers, capping it below 1.25, and require these facilities to enter into renewable energy power purchase agreements (PPAs) to avoid reliance on coal-fired grid backup during dry seasons. Regarding tourism, emissions can be reduced by accelerating the deployment of integrated "transport-tourism" clean energy networks, such as replacing all scenic spot shuttle buses with electric vehicles and subsidizing low-carbon regional aviation. For these ecologically fragile zones, the strategy should not simply replicate the industrialization path of the eastern regions but instead leverage their renewable energy advantages to develop a "low-carbon plus" service economy.

Strengthen the synergistic governance of SDG7 and economic planning to curb high-carbon urbanization. To address the limitations of single-dimensional energy transitions, the YREB must shift from "relative" to "absolute" control targets. Dynamic regulatory thresholds should be incorporated into local government evaluation systems, linking performance metrics not only to GDP growth but also to the decoupling rate of energy intensity. Furthermore, given the inertia of population and energy structure drivers identified in the midstream region, long-term spatial planning should optimize urban agglomeration layouts to prevent low-density sprawl. Specifically, new urban infrastructure projects—such as large-scale housing and transportation networks—driven by population inflows in midstream metropolitan areas (e.g., Wuhan) must comply with mandatory green building standards and utilize low-carbon building materials. This approach ensures that urbanization in the midstream and upstream regions does not replicate the high-carbon footprint characteristic of early downstream development.

## 7 Limitations and future prospects

This study acknowledges several limitations. First, due to data availability, the calculation of carbon sinks focused primarily on forest ecosystems, excluding the potential contributions of soil, wetlands, and croplands. Second, the energy structure was approximated by the proportion of renewable electricity generation, which may not fully capture the decarbonization of heating and industrial fuel use. Future research should aim to incorporate multisource sink data and more granular energy consumption metrics to improve the accuracy of regional CFP assessments. Although our analysis reveals a significant temporal correlation between the "M-shaped" fluctuation of the SR coefficient and China's Five-Year Plan policy cycles, the current analytical framework cannot fully isolate these policy effects from concurrent confounding factors such as macroeconomic cycles, industrial migration, and price shocks. Future studies could build upon our findings by introducing quantitative policy intensity indicators or employing quasi-experimental methods, such as Difference-in-Differences (DID) or event study frameworks, to achieve more precise causal identification of specific policy interventions.

## Data availability statement

The original contributions presented in the study are included in the article/Supplementary Material, further inquiries can be directed to the corresponding author.

## Author contributions

XF: Software, Writing – original draft, Methodology, Conceptualization. KL: Visualization, Data curation, Formal Analysis, Writing – original draft, Conceptualization. LY: Writing – original draft, Formal Analysis. TS: Formal Analysis, Writing – original draft. TW: Writing – review and editing, Data curation, Project administration, Visualization.

## Funding

The author(s) declared that financial support was received for this work and/or its publication. This research was funded by the Social Science Foundation of Jiangsu Province, grant number 24EYB005.

## Conflict of interest

The author(s) declared that this work was conducted in the absence of any commercial or financial relationships that could be construed as a potential conflict of interest.

## Generative AI statement

The author(s) declared that generative AI was not used in the creation of this manuscript.

## Publisher's note

## Supplementary material

The Supplementary Material for this article can be found online at: https://www.frontiersin.org/articles/10.3389/fenvs.2026.1764762/full#supplementary-material

## References

Bao, C., and Xu, M. (2019). Cause and effect of renewable energy consumption on urbanization and economic growth in China's provinces and regions. *J. Clean. Prod.* 231, 483–493. doi:10.1016/j.jclepro.2019.05.191

Charles, V., and Emrouznejad, A. (2024). DEA-based index systems for addressing the United Nations' SDGs. *Environ. Sci. Policy* 162, 103950. doi:10.1016/j.envsci.2024.103950

Chen, J., Fan, W., Li, D., Liu, X., and Song, M. (2020). Driving factors of global carbon footprint pressure: based on vegetation carbon sequestration. *Appl. Energy* 267, 114914. doi:10.1016/j.apenergy.2020.114914

Chen, C., Luo, Y., Zou, H., and Huang, J. (2023). Understanding the driving factors and finding the pathway to mitigating carbon emissions in China's Yangtze River Delta region. *Energy* 278, 127897. doi:10.1016/j.energy.2023.127897

Fan, W., Huang, S., Yu, Y., Xu, Y., and Cheng, S. (2022). Decomposition and decoupling analysis of carbon footprint pressure in China's cities. *J. Clean. Prod.* 372, 133792. doi:10.1016/j.jclepro.2022.133792

Gössling, S., and Peeters, P. (2015). Assessing tourism's global environmental impact 1900-2050. *J. Sustain. Tour.* 23 (5), 639–659. doi:10.1080/09669582.2015.1008500

Grossman, G. M., and Krueger, A. B. (1995). Economic growth and the environment. *Q. J. Econ.* 110, 353–377. doi:10.2307/2118443

Guo, L., Ma, Z. H., and Zhang, L. J. (2008). Comparison of bandwidth selection in application of geographically weighted regression: a case study. *Can. J. For. Res.* 38 (9), 2526–2534. doi:10.1139/x08-091

Han, C., Zhang, W. G., and Feng, Z. B. (2017). How does environmental regulation remove resource misallocation? An analysis of the first obligatory pollution control in China. *China Ind. Econ.* 4, 115–134. doi:10.19581/j.cnki.ciejournal.2017.04.007

Huang, B., Wu, B., and Barry, M. (2010). Geographically and temporally weighted regression for modeling spatio-temporal variation in house prices. *Int. J. Geogr. Inf. Sci.* 24 (3), 383–401. doi:10.1080/13658810802672469

Huang, Y., Yu, Q., and Wang, R. (2021). Driving factors and decoupling effect of carbon footprint pressure in China: based on net primary production. *Technol. Forecast. Soc. Chang.* 167, 120722. doi:10.1016/j.techfore.2021.120722

Huang, H., Jia, J., Liu, S., and Chen, D. (2023). Analysis of spatial-temporal evolution and influencing factors of carbon sinks in Yangtze River Economic Belt from 2000 to 2020. *Res. Environ. Sci.* 36, 1564–1576. doi:10.13198/j.issn.1001-6929.2023.06.16

Liang, D., Lu, H., Guan, Y., and Feng, L. (2022). Drivers for decoupling carbon footprint pressure from economic growth in China's provinces. *Geogr. Sustain.* 3, 258–267. doi:10.1016/j.geosus.2022.08.003

Luchman, J. N. (2021). Determining relative importance in Stata using dominance analysis: domin and domme. *Stata J. Promot. Communications Statistics Stata* 21, 510–538. doi:10.1177/1536867X211025837

Luo, Z., and Qi, B. C. (2021). The effects of environmental regulation on industrial transfer and upgrading and banking synergetic development: evidence from water pollution control in the Yangtze River Basin. *Econ. Res. J.* 56 (2), 174–189.

Ma, X., Wang, C., Dong, B., Gu, G., Chen, R., Li, Y., et al. (2019). Carbon emissions from energy consumption in China: its measurement and driving factors. *Sci. Total. Environ.* 648, 1411–1420. doi:10.1016/j.scitotenv.2018.08.183

Song, M., Chang, L., and Hao, X. (2021). Analysis on the spatio-temporal evolution and driving factors of carbon pressure in the middle reaches of the Yangtze River. *J. Environ. Econ.* 6, 23–40. doi:10.19511/j.cnki.jee.2021.02.003

Tian, L., Chai, J., Zhang, X., and Pan, Y. (2024). Spatiotemporal evolution and driving factors of China's carbon footprint pressure: based on vegetation carbon sequestration and LMDI decomposition. *Energy* 310, 133299. doi:10.1016/j.energy.2024.133299

Wang, X. B., and Xu, T. J. (2022). A study of the environmental target constraints on enterprise productivity. *Econ. Sci.* 5, 78–94. doi:10.12088/PKU.jjkx.2022.05.06

Wang, J., Zhang, S., and Zhang, Q. (2021). The relationship of renewable energy consumption to financial development and economic growth in China. *Renew. Energy* 170, 897–904. doi:10.1016/j.renene.2021.02.038

Wang, Z., Zhao, Z., and Wang, C. (2021). Random forest analysis of factors affecting urban carbon emissions in cities within the Yangtze River Economic Belt. *PLoS One* 16 (6), e0252337. doi:10.1371/journal.pone.0252337

Wu, C. Q., and Deng, M. L. (2018). Agglomeration features and influencing factors of high energy-consuming industries in the Yangtze River Economic Belt. *Sci. and Technol. Prog. Policy* 35 (16), 67–74. doi:10.6049/kjjbydc.2017120191

Wu, Y., Xu, Y., Tang, Y., Jia, N., Li, W., Li, C., et al. (2023). Temporal and spatial characteristics of net CO2 emissions and decoupling analysis in Yangtze River Economic Belt. *Environ. Sci.* 44, 1258–1266. doi:10.13227/j.hjkx.202203155

Xie, X. M., Han, Y. H., and Tan, H. (2024). Greening China's digital economy: exploring the contribution of the East-West computing resources transmission Project to CO2 reduction. *Hum. Soc. Sci. Commun.* 11 (1), 466. doi:10.1057/s41599-024-02963-0

Yang, S. J., Wang, Y. J., Han, R. Q., Chang, Y., and Sun, X. H. (2021). Spatial heterogeneity of factors influencing CO2 emissions in China's high-energy-intensive industries. *Sustainability* 13 (15), 8304. doi:10.3390/su13158304

York, R., Rosa, E. A., and Dietz, T. (2002). Bridging environmental science with environmental policy: plasticity of population, affluence, and technology. *Soc. Sci. Q.* 83, 18–34. doi:10.1111/1540-6237.00068

Zhang, H., and Lei, Y. D. (2023). Study on spatial and temporal characteristics and influencing factors of carbon emissions in the urban agglomeration of the middle reaches of the Yangtze River. *Sustainability* 15 (13), 10176. doi:10.3390/su151310176